REPORT DOCUMENTATION PAGE

Form Approved
OMB No. 0704-0188

1. REPORT DATE *(DD-MM-YYYY)*	2. REPORT TYPE	3. DATES COVERED *(From - To)*
	Technical Papers	

4. TITLE AND SUBTITLE

5a. CONTRACT NUMBER

5b. GRANT NUMBER

5c. PROGRAM ELEMENT NUMBER

6. AUTHOR(S)

5d. PROJECT NUMBER
2302

5e. TASK NUMBER
M1G2

5f. WORK UNIT NUMBER

7. PERFORMING ORGANIZATION NAME(S) AND ADDRESS(ES)

Air Force Research Laboratory (AFMC)
AFRL/PRS
5 Pollux Drive
Edwards AFB CA 93524-7048

8. PERFORMING ORGANIZATION REPORT

9. SPONSORING / MONITORING AGENCY NAME(S) AND ADDRESS(ES)

Air Force Research Laboratory (AFMC)
AFRL/PRS
5 Pollux Drive
Edwards AFB CA 93524-7048

10. SPONSOR/MONITOR'S ACRONYM(S)

11. SPONSOR/MONITOR'S NUMBER(S)

12. DISTRIBUTION / AVAILABILITY STATEMENT

Approved for public release; distribution unlimited.

13. SUPPLEMENTARY NOTES

14. ABSTRACT

15. SUBJECT TERMS

16. SECURITY CLASSIFICATION OF:			17. LIMITATION OF ABSTRACT	18. NUMBER OF PAGES	19a. NAME OF RESPONSIBLE PERSON
a. REPORT	b. ABSTRACT	c. THIS PAGE			Leilani Richardson
Unclassified	Unclassified	Unclassified	A		19b. TELEPHONE NUMBER *(include area code)* (661) 275-5015

3k separate items are enclosed

MEMORANDUM FOR PRS (In-House /Contractor Publication)

FROM: PROI (TI) (STINFO)

21 October 1999

SUBJECT: Authorization for Release of Technical Information, Control Number: **AFRL-PR-ED-TP-1999-0195**
Smith, C.W.; Gloss, K.T., Liu, C.T, "Test Geometries for Bondline Cracked Photoelastic Models; Preliminary Results" (Paper)

ASME 1999 Mechanical Engineering Congress and Exposition **(Statement A)**

Item Ci

TEST GEOMETRIES FOR BONDLINE CRACKED PHOTOELASTIC MODELS; PRELIMINARY RESULTS

C. W. Smith and K. T. Gloss
Dept. of Engineering Science and Mechanics
Va. Poly. Inst. and State University
Blacksburg, VA 24061

C. T. Liu
Air Force Research Laboratory
Edwards AFB, CA 93524-7680

ABSTRACT

By interrogating polyurethane specimens containing bondlines with cracks photoelastically, the authors are conducting a study of the effect of fixed ends upon the stress intensity factor (SIF) for double edge cracked specimens for test specimens of relatively short height. Preliminary results suggest that, while the presence of the bondline increases the SIF with increasing crack length, reducing the specimen height will reduce the SIF level for all crack lengths.

INTRODUCTION

Solid propellant is a particulate composite, consisting of hard polyhedral particles embedded in a soft rubber matrix. When bonded to a rubber liner, the joint may be subject to cracking along the bondline. Except to very low temperatures, the material behaves as a very soft material with substantial crack tip blunting. When the hard particles dewet allowing the soft matrix to produce severe blunting of the crack tip, the crack will then resharpen by joining with voids developed by dewetting along and ahead of the crack front. The process of blunt-growth-blunt-growth becomes a highly nonlinear process. Numerical analysts often attempt to smooth out the process by linearizing the problem into one with slow, steady growth.

Optical grade polyurethane is a transparent, soft, linear material which approximately simulates a linearized propellant material during crack opening and growth. For this reason, it was selected to study the interactive effects of boundaries and bondlines on the stress intensity factors (SIFs) of bondline cracks. It has been established that, because of the soft nature of propellant near room temperature and above, long single edge cracked specimens tend to undergo significant bending.

ANALYTICAL AND EXPERIMENTAL CONSIDERATIONS

For the present study, a double edge cracked bonded specimen was selected with cracks in the bondline to reduce the bending effect and experimental results have been obtained for both square specimens (for which an analytical solution (Bowie, 1964) is available with no bondline present) and specimens with shorter heights. The Bowie solution for square, double edge cracked specimens with no bondline, which employed conformal mapping has been found accurate above crack length to half width ratios of 0.2.

It was considered important to produce an accurate through the thickness crack front with a rounded tip to simulate blunting and a razor blade was em-

ployed to produce the crack. In order to account for any effects due to tip blunting and specimen thickness, a test was run on a homogeneous single edge cracked polyurethane specimen (E = 4.70 MPa) (Fig. 1) and the results were compared to a boundary collocation two dimensional (2D) solution (Gross, Srawley and Brown, 1964, also Srawley and Brown, 1967) and the SIF was determined using a two parameter algorithm from Appendix A (Smith and Kobayashi, 1987) which has been widely employed on photoelastic data. While this algorithm was developed for application to a homogeneous material without a bondline, it is expected to be reasonably accurate for bondline work here since for plane strain states in incompressible materials, the interface fracture theory reduces to the homogeneous case for loads away from the crack tip (Hutchinson and Suo, 1992). Results from the single edge crack test indicated that the experimental result was 7.8% higher than the boundary collocation plane stress solution. This value will be used to correct subsequent test data to plane stress solutions for double edge cracks.

TESTS ON SPECIMENS WITH DOUBLE EDGE CRACKS IN THE BONDLINE

A series of polyurethane test specimens (Fig. 2) were prepared with double edge cracks in the bondline for both square specimens and some with the specimen height reduced by half. Specimen ends were inserted into grooves in aluminum plates and bonded to simulate methods used for bonding solid propellant material specimens. The extent to which this method achieves a uniform axial stress field in the direction of the load will be shown by global stress fringe photographs of the test specimens under load. The analytical models also assume zero transverse displacement of the test specimen at the boundaries. Companion tests were run for different crack lengths as shown in Fig. 2. These specimens were made by fitting the adherends to teflon coated razor blades on each side of the specimen and then pouring an adhesive which chemically matched the polyurethane adherends into the opening in between and then curing at 160° F. for 12 hrs., after which the razor blades were removed. It had been previously found (Smith, Finlayson and Liu, 1998) that modulus mismatch exerted negligible effect upon the SIF values for the cracks within the bondline for modulus ratios not exceeding about 3.5 so no modulus mismatch was introduced into the models.

Figs. 3a and 3b are global fringe photos of the square and short specimens respectively under load. They reveal some irregularities along the fixed edges possibly due to adhesive slippage. This results in slight dysymmetry of the near tip fringe patterns but the effect on K_1 is well within the expected experimental scatter of $\pm$ 5%. This effect was accommodated by averaging the K_1 values for the two cracks in each specimen. Figs 4a and 4b show that the near tip fringe patterns show no rotation of the fringe loops which suggest the absence of any shear mode K_2. The data zones for K_1 determination in Figure 4 are taken along a line normal to the crack plane and passing through the tip of the crack. The data zone locations are indicated. The dark bands surrounding the crack opening in Fig. 4. are part of the crack surface which turns outward due to increased crack opening at the near surface of the specimen.

RESULTS

Using the near tip fringe pattern photos, the algorithm described in Appendix A was used to extract

K_1 values from the local fringe pattern data. An example of the procedure is given in Fig. A-2. K_1 values were computed both above and below the bondline and agreed to well within experimental scatter of 5%. A summary of the test data and results are found in Table 1.

A plot of the results for the square and short specimen test data are presented in Fig. 5. Also shown is the theoretical solution for the double edge crack with no bondline due to Bowie (1964). The experimental data are corrected for thickness and Poisson Ratio ($\nu = 0.5$) effects for comparison with Bowie's solution. Two results are apparent: i) As a/b increases, the SIF increases faster for a crack in the bondline than for a crack in a homogeneous material and ii) Reducing the height of the double edge cracked specimens reduces the SIF level for all a/b ratios studied to date.

The reasons for the two above noted observed behaviors have not been experimentally investigated. Consequently, at this stage in our study, we can only conjecture as to why the above noted departures from the behavior of homogeneous specimens occurred.

For the case of the more rapid increase in SIF with crack depth in the bonded cracked specimens than for the homogeneous ones, it may be that when the bondline adhesive cures between the adherends, an added constraint is developed in the crack tip region, producing a stiffer response.

The reduction in the SIF level for all crack sizes examined thus far which occurs when the specimen height is reduced may result from the constraint which the fixed ends exert upon the crack opening tendencies of the material behind the crack tips.

It is intended to extend the cracks toward a/b = 0.5 and beyond since this is the region of greatest rate of increase in SIF with increasing a/b. These studies are underway.

ACKNOWLEDGMENT

The authors wish to thank the Air Force Research Laboratory for support of this work through Sparta Inc. under sub-contract No. 98-522.

REFERENCES

Bowie, O. L., "Symmetric Edge Cracks in Tensile Sheet with Constrained Ends," *Journal of Applied Mechanics*, pp. 726-728, Dec. (1964).

Gross, B., Srawley, J. E., and Brown, W. F., "Stress Intensity Factors for a Single-Edge Notch Tensile Specimen by Boundary Collocation of a Stress Function," *Tech. Note D-2395 NASA*, 11 pages, Aug. (1964).

Hutchinson, J. W. and Suo, H., "Mixed Mode Cracking in Layered Materials," *Advances in Applied Mechanics*, V. 29 New York, Academic Press, pp. 63-91, (1992).

Smith, C. W., and Kobayashi, A. S., "Experimental Fracture Mechanics," In: Kobayashi, A. S., Ed. *Handbook on Experimental Mechanics* 2nd Ed., VCH New York, pp. 905-968, (1993).

Smith, C. W., Finlayson, E. F., and Liu, C. T., "Influence of Material Properties on SIF's Determined by Frozen Stress," *Journal of Engineering Fracture Mechanics*, V. 61, N 5/6, pp. 555-568, (1998)

Srawley, J. E. and Brown, W. F., "Plane Strain Crack Toughness Testing of High Strength Metallic Materials," ASTM STP No. 410 (1967).

APPENDIX A

(Mode I Algorithm)

Beginning with the Griffith-Irwin Equations, we may write, for Mode I, for the homogeneous case,

$$\sigma_{ij} = \frac{K_1}{(2\pi r)^{\frac{1}{2}}} f_{ij}(\theta) + \sigma^{\circ}_{ij} \qquad (i.j. = n, z) \quad (1)$$

where:

σ_{ij} are components of stress,

K_1 is SIF,

r, θ are measured from crack tip(Fig. A-1),

σ°_{ij} are nonsingular stress components.

Then, along $\theta = \pi/2$ the direction of greatest local fringe spreading, after truncating σ_{ij}

$$(\tau_{nz})_{max} = \frac{K_1}{(8\pi r)^{\frac{1}{2}}} + \tau^{\circ} = \frac{K_{AP}}{(8\pi r)^{\frac{1}{2}}} \qquad (2)$$

where $\tau^{\circ} = f(\sigma^{\circ}_{ij})$ and is constant over the data range, K_{AP} = apparent SIF, $(\tau_{nz})_{max}$ = maximum shear stress in nz plane

$$\therefore \frac{K_{AP}}{\bar{\sigma}(\pi a)^{\frac{1}{2}}} = \frac{K_1}{\bar{\sigma}(\pi a)^{\frac{1}{2}}} + \frac{\sqrt{8}\tau^{\circ}}{\bar{\sigma}} \left(\frac{r}{a}\right)^{\frac{1}{2}} \qquad (3)$$

where (Fig. A-1) a = crack length, and $\bar{\sigma}$ = remote normal stress

$$i.e. \frac{K_{AP}}{\bar{\sigma}(\pi a)^{\frac{1}{2}}} \text{ vs. } \sqrt{\frac{r}{a}} \text{ is linear.}$$

Since from the Stress-Optic Law:

$$(\tau_{nz})_{max} = \frac{nf}{2t} \text{ where}$$

n = stress fringe order

f = material fringe value

t = specimen thickness

and from Eq. 2

$$K_{AP} = \tau^{max}_{nz}(8\pi r)^{\frac{1}{2}} = \frac{nf}{2t}(8\pi r)^{\frac{1}{2}},$$

then K_{AP} (through a measure of n) and r becomes the measured quantity from the stress fringe pattern at different points in the pattern.

A typical plot of normalized K_{AP} vs. $\sqrt{r/a}$ for a cracked, bonded specimen is shown in Fig. A-2.

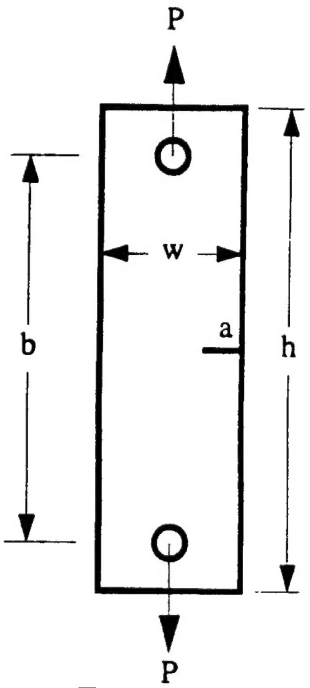

w = 38.1 mm
t = 12.7 mm
h = 127 mm
b = 102 mm
P = 2.74 kgs

		(MPa $\sqrt{m}$)		
a (mm)	a/w	K_{exp}	K_{th}^{*}	% difference
7.54	0.20	12.76	11.84	7.80

* Srawley and Brown, 1967

Fig. 1 Single Edge Crack Results for Artificial Cracks

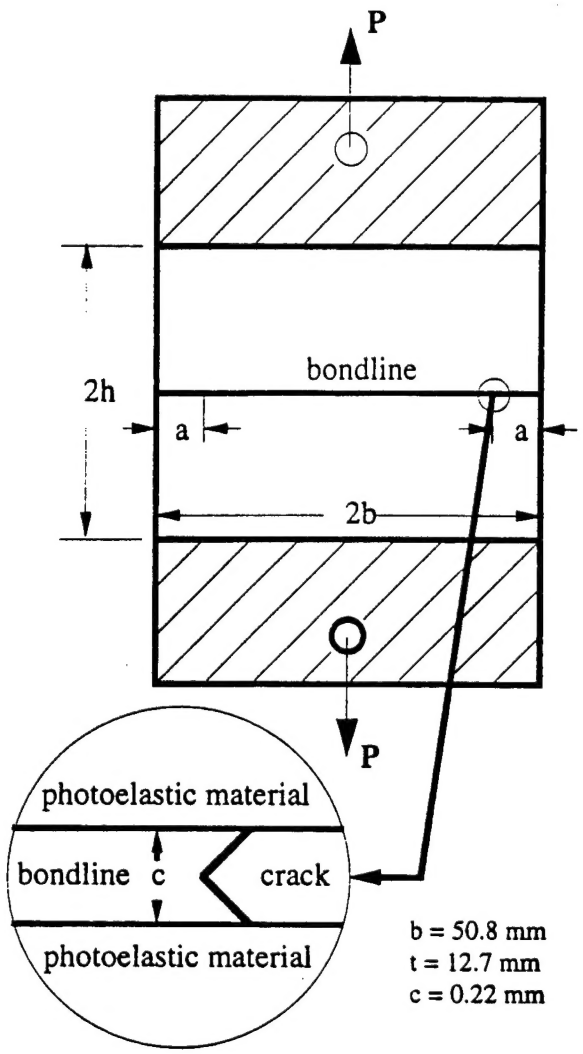

test	a (mm)	h (mm)	a/b	P (kg)
DS2	12.7	50.8	0.25	7.64
DS3	17.4	50.8	0.34	7.64
DS4	20.6	50.8	0.41	7.64
DS5	25.4	50.8	0.50	7.64
DS6	12.7	25.4	0.25	7.64
DS7	17.4	25.4	0.34	5.37
DS8	20.6	25.4	0.41	5.17
DS9	25.4	25.4	0.50	5.17

Fig. 2 Bonded Specimens with Double Edge Bondline Cracks

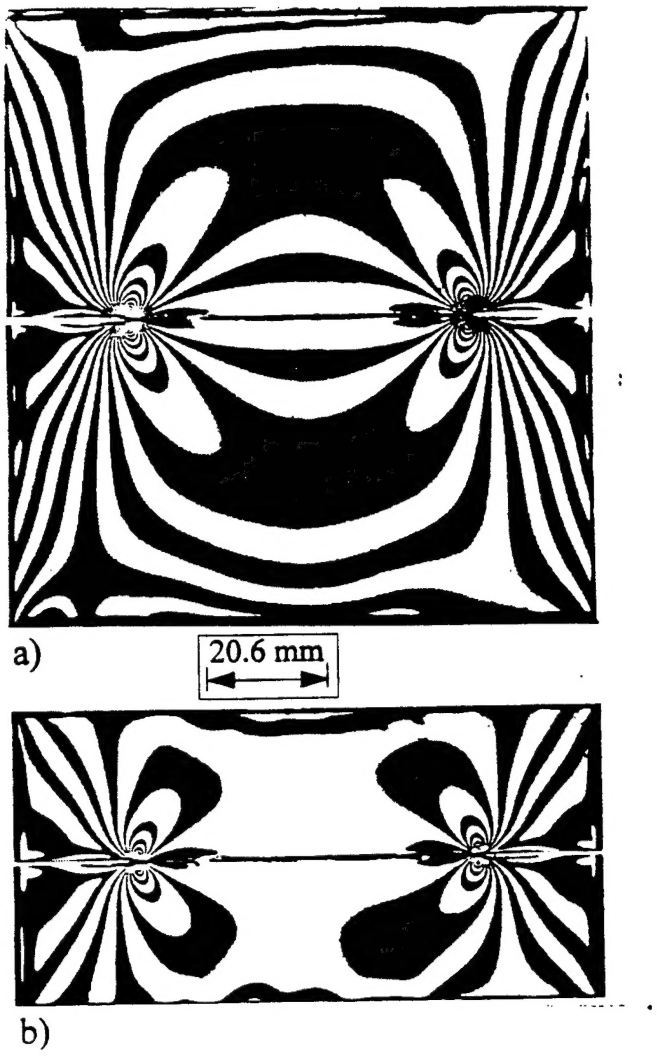

Fig. 3+: Global Stress Fringe Patterns for a) Square Specimen, b) Short Specimen.

+All fringe patterns have a bright background, (i.e. integral fringes are white, half fringes are black).

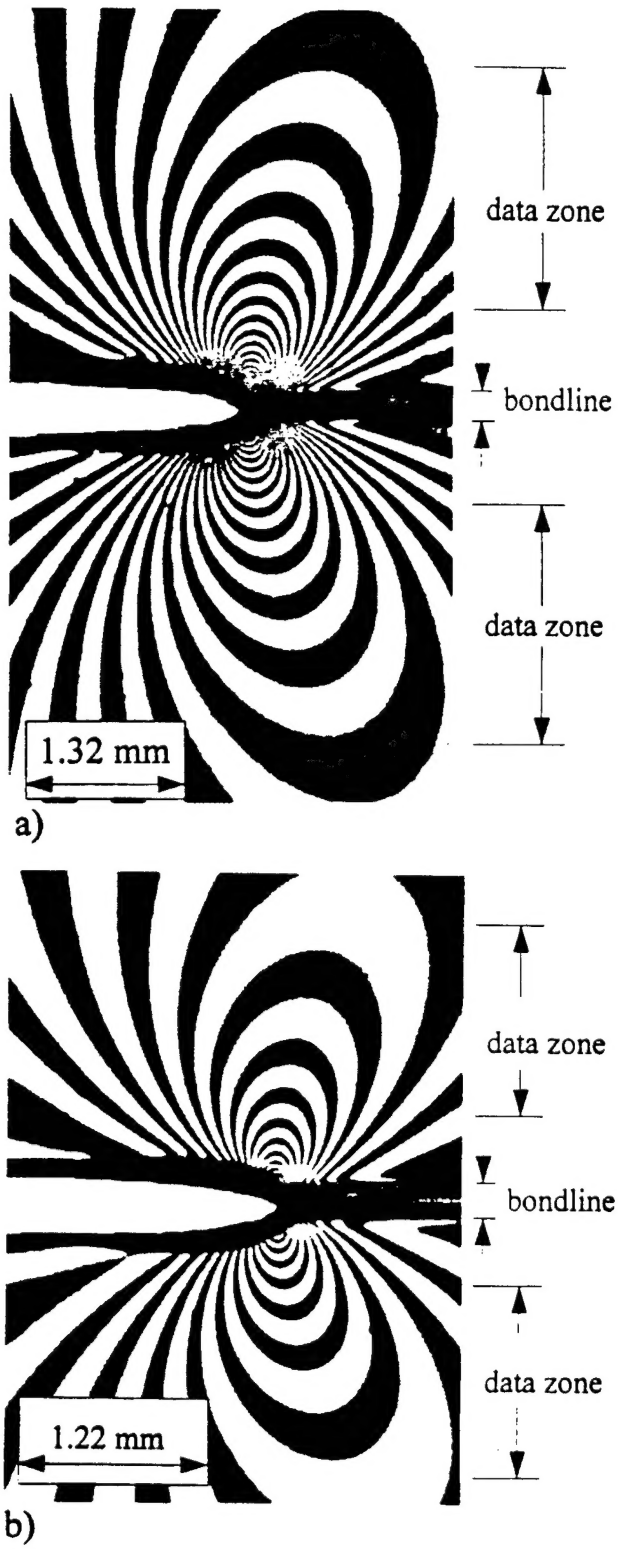

Fig. 4+: Local Stress Fringe Patterns for a) Square Specimen, b) Short Specimen.

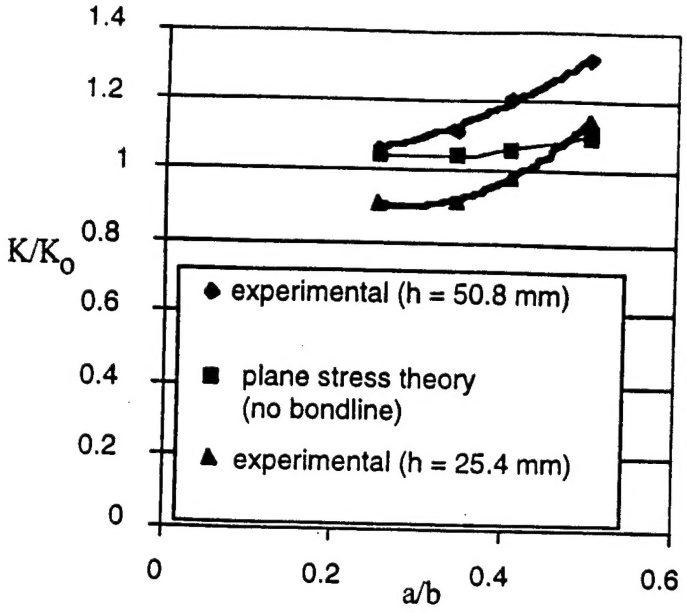

Fig. 5: Comparison of Bondline Crack Test Results with Double Edge Crack Results for Homogeneous Double Edge Crack Theory.

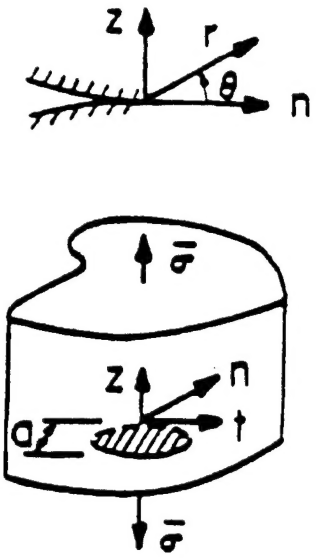

Fig. A-1 Mode I Notation

TABLE 1

name	a/b	P (kg)	exp. K/Ko	exp. corr. (ν = 0.5) K/Ko	Bowie* (ν = 0.3) K/Ko
DS2	0.25	7.64	1.15	1.06	1.04
DS3	0.34	7.64	1.21	1.11	1.04
DS4	0.41	7.64	1.31	1.20	1.06
DS5	0.50	7.64	1.43	1.32	1.10
DS6	0.25	7.64	0.98	0.91	—
DS7	0.34	5.37	0.99	0.91	—
DS8	0.41	5.17	1.06	0.99	—
DS9	0.50	5.17	1.24	1.14	—

* - plane stress, no bondline $K_o = \sigma_o\sqrt{\pi a}$

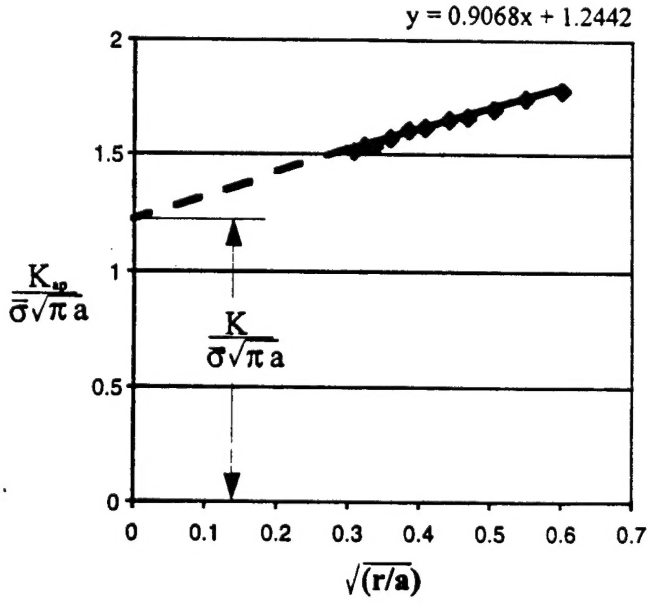

Fig. A-2: Determination of K_I from Test Data for DS3.